

## **Numerical simulation of mass transfer and convection near a hydrogen bubble during water electrolysis in a magnetic field**

Mutschke, G.; Fröhlich, J.; Yang, X.; Eckert, K.; Karnbach, F.; Uhlemann, M.;  
Baczyszmaliski, D.; Cierpka, C.;

Originally published:

May 2017

**Magnetohydrodynamics 53(2017)1, 193-199**

Perma-Link to Publication Repository of HZDR:

<https://www.hzdr.de/publications/Publ-23656>

Release of the secondary publication  
on the basis of the German Copyright Law § 38 Section 4.

# NUMERICAL SIMULATION OF MASS TRANSFER AND CONVECTION NEAR A HYDROGEN BUBBLE DURING WATER ELECTROLYSIS IN A MAGNETIC FIELD

*G. Mutschke*<sup>1,2</sup>, *D. Baczyzmalski*<sup>3</sup>, *C. Cierpka*<sup>4</sup>, *F. Karnbach*<sup>2,5</sup>,  
*M. Uhlemann*<sup>5</sup>, *X. Yang*<sup>1,2</sup>, *K. Eckert*<sup>1,2</sup>, *J. Fröhlich*<sup>2</sup>

<sup>1</sup> *Helmholtz-Zentrum Dresden-Rossendorf,  
PO Box 510119, D-01314 Dresden, Germany*

<sup>2</sup> *Technische Universität Dresden, D-01062 Dresden, Germany*

<sup>3</sup> *Universität der Bundeswehr München, D-85577 Neubiberg, Germany*

<sup>4</sup> *Technische Universität Ilmenau, D-99693 Ilmenau, Germany*

<sup>5</sup> *IFW Dresden, D-01069 Dresden, Germany*

*e-Mail: g.mutschke@hzdr.de*

Numerical simulations are presented resolving in detail local phenomena near a single hydrogen bubble at the cathode during the electrolysis of water. The modelling is based on recent experiments on hydrogen evolution at a platinum micro-electrode. The simulation results provide local insight into electrolyte convection, species concentration and mass transfer during electrolysis, and the influence of the Lorentz force caused by a vertical magnetic field on the bubble departure is discussed.

**Introduction.** Hydrogen produced from wind or solar power could be used easily for storing energy also at large scale. However, when splitting water by electrolysis, with increasing current density, the impact of bubble coverage and gas void fraction on electrical losses becomes more pronounced, and the cell efficiency decreases. Forcing of electrode-parallel convection is well-known to reduce the fractional bubble coverage by enhancing the bubble detachment. Beside electrolyte pumping and a vertical orientation of the electrodes to take benefit from buoyancy, additional support to advance the release of gas bubbles would be desirable. Here, magnetic fields appear to be attractive, as proper Lorentz forces can be generated by utilizing the current density available in the cell, anyway. While electrode-parallel fields can be expected to add additional shear supporting the bubble release [1, 2, 10, 13], the effect of an electrode-normal magnetic field on the bubble departure is discussed controversially in the literature. Koza *et al.* observed advanced hydrogen desorption at macro-electrodes [3], whereas Fernandez *et al.* reported a stabilizing effect at micro-electrodes [4]. Recent experiments and numerical simulations of Liu *et al.* at micro-electrodes also show that a vertical magnetic field seems to retard the bubble release [5]. The azimuthal Lorentz force (see Fig. 2) leads to a strong azimuthal flow, and the resulting pressure change is suspected to be responsible for the bubble stabilization. However, Weier *et al.* have estimated recently that at a macro-electrode this influence is rather weak [6].

In general, a detailed look at local phenomena near single bubbles at the electrode might be useful to improve the understanding of the bubble departure which is of interest for electrochemical processes with gas evolution in general as, e.g., plating of ferrous materials. Micro-electrodes are especially attractive in experiments to control the place of nucleation and bubble growth [7, 8]. On the other hand, numerical simulation can easily give insight into the local and temporal behavior of electrolyte convection, species concentration and mass transfer during

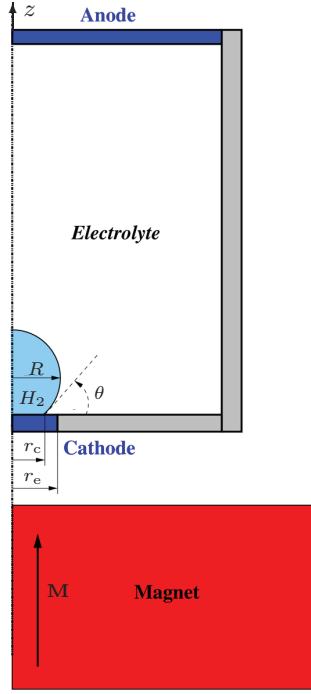
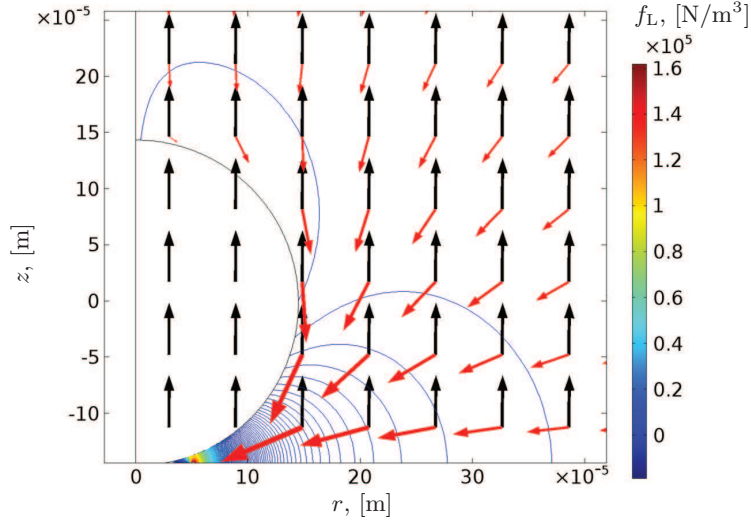


Fig. 1. Sketch of the cylindrical cell in the  $(r, z)$ -plane. The scales are modified for better visibility. The vector  $\mathbf{M}$  shows the direction of magnetization of the NdFeB magnet.

electrolysis [4, 9]. The following simulations of electrolysis at a micro-electrode in a vertical magnetic field are intended to contribute to the current discussion on the influence of the Lorentz force on the departure behavior of bubbles from the electrode.

**1. Presentation of the problem.** Recently, measurements of the electrolyte convection around a single hydrogen bubble evolving at a micro-electrode under the influence of a vertical magnetic field were made [11]. For gaining additional insight, corresponding numerical simulations are undertaken. A cylindrical cell is used, which allows for azimuthal symmetry in the simulations, thereby closely matching the geometry of the cuboid cell used in the experiment. A sketch of the cell is shown in Fig. 1. The radial and the vertical extension of the cell ( $R_r = 5.6 \text{ mm}$  and  $R_z = 45 \text{ mm}$ ) are much larger than the size of the micro-electrode (cathode) on the bottom ( $r_e = 50 \mu\text{m}$ ). The electrolyte consists of a  $1 \text{ M H}_2\text{SO}_4$  solution. The steady simulations performed describe an early stage of the periodic bubble cycle ( $\tau = 0.15$ , with  $\tau$  being the normalized bubble cycle time) at a cell potential of  $E = -1.5 \text{ V}$  vs. MSE reference electrode, corresponding to a cell current of  $1 \text{ mA}$ . According to the experiment, a hydrogen bubble of radius  $R = 145 \mu\text{m}$  is attached to the cathode with a contact angle of  $\theta = 9^\circ$ . As the characteristic Eötvös number amounts to  $\text{Eo} \approx 10^{-2}$  [14], a circular bubble shape is assumed, and the part of the electrode covered by hydrogen easily follows (the radius of contact is  $r_c = 22.7 \mu\text{m}$ ). Below the bottom of the cell, a large cylindrical NdFeB permanent magnet is arranged ( $R_M = 22.57 \text{ mm}$ ,  $H_M = 20 \text{ mm}$ ) which is magnetized in the vertical direction. The distance between the upper surface of



*Fig. 2.* Color isolines of the azimuthal Lorentz force (maximum value shown restricted by hand) resulting from the bending of the current density (red arrows, logarithmic scaling) and the magnetic field (black arrows) in the vicinity of the hydrogen bubble. Simulation result in the  $(r, z)$ -plane.

the magnet and the cathode surface is 14 mm. As the dimensions of the magnet are large compared to the cell radius and of course also to the bubble size, in the vicinity of the hydrogen bubble a nearly constant magnetic field is expected which is oriented almost perfectly in the vertical direction (see Fig. 2).

**2. Numerical model.** The process of water electrolysis is assumed to take place in an aqueous electrolyte of constant electrical conductivity  $\sigma$ . With a non-conductive hydrogen bubble, the resulting primary current density  $\mathbf{j}$  in the electrolyte can be determined by solving a Laplace equation for the electric potential  $\Phi$ :

$$\Delta\Phi = 0, \quad \mathbf{j} = \sigma\nabla\Phi. \quad (1)$$

For potentiostatic operation, the respective boundary conditions at the electrodes can be set such as to match a desired cell current. Hereby, at the cathode, only the wetted part is to be used (see Fig. 1). The temporal evolution of the concentration  $c$  of hydrogen being dissolved in the electrolyte can be described by a convection-diffusion equation

$$\frac{\partial c}{\partial t} + (\mathbf{u}\nabla) c = D\Delta c. \quad (2)$$

Here,  $\mathbf{u}$  and  $D$  denote the velocity vector of the electrolyte and the diffusion coefficient of the dissolved hydrogen, respectively. The distribution of the current density at the wetted part of the cathode is used to define the boundary flux describing the production rate of dissolved hydrogen. Using Faradays law, it reads

$$\frac{\partial c}{\partial n} = \frac{1}{zFD} j_n \quad (3)$$

where  $n$ ,  $z$  and  $F$  indicate the electrode-normal direction, the charge number and the Faraday constant, respectively. The boundary condition at the bubble interface was defined according to thermodynamic equilibrium by using Henrys law. At the passive walls of the cell, a concentration of zero was applied. The convection of the electrolyte is determined by the incompressible Navier-Stokes equation in

conjunction with the incompressibility constraint:

$$\rho_0 \left( \frac{\partial \mathbf{u}}{\partial t} + (\mathbf{u} \cdot \nabla) \mathbf{u} \right) = -\nabla p + \eta \Delta \mathbf{u} + \mathbf{f}_B + \mathbf{f}_L, \quad \Delta \cdot \mathbf{u} = 0. \quad (4)$$

The volume forces taken into account are the buoyancy force  $\mathbf{f}_B$  due to solutal changes of electrolyte density within the Boussinesq approximation and the Lorentz force  $\mathbf{f}_L$  due to the cross product of cell current and magnetic field:

$$\mathbf{f}_B = \rho_0 \beta_c (c - c_0) \mathbf{g}, \quad \mathbf{f}_L = \mathbf{j} \times \mathbf{B}. \quad (5)$$

Here,  $\beta_c$  denotes the linear volume expansion coefficient.

Due to azimuthal symmetry, all simulations can be restricted to the  $(r, z)$ -plane of the radial and of the vertical coordinate. The magnetic field  $\mathbf{B}$  was determined from solving the respective magnetostatic problem with the magnet region of constant vertical magnetization in a half-circular domain much larger than the cell to avoid influence from the finite distance of the outer boundary. The radial and vertical components of the magnetic field and the current density

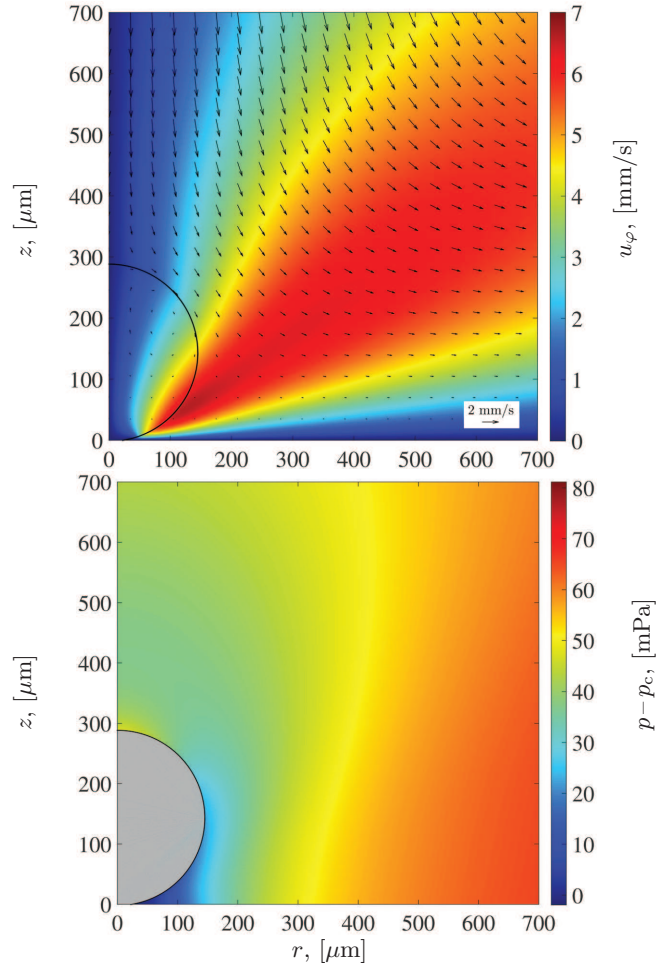


*Fig. 3.* Top: Color surface of the azimuthal velocity and vectors of the meridional velocity. Bottom: Related pressure distribution (reference pressure  $p_c$ ). (Reproduced from [11] with permission. Copyright 2016, The Electrochemical Society).

give rise to an azimuthal ( $\varphi$ ) component of the Lorentz force only:

$$\mathbf{f}_L \cdot \mathbf{e}_\varphi = B_r j_z - B_z j_r. \quad (6)$$

The Navier-Stokes equations (4) also apply to the bubble region, where proper material constants of the hydrogen gas have to be used. At the liquid-gas interface, either a no-slip or a slip condition can be applied, the latter allowing the interface and the gas inside the bubble to move. The simulations were performed using Comsol V.4.4 with an unstructured grid of triangular elements. During resolution studies, the grid was properly refined near the bubble interface, the cathode and the magnet edges, where large gradients of the calculated quantities occur. The final grid consists of about 50 000 elements, with an element size at, e.g., the cathode of about  $1 \mu\text{m}$ . The fully-coupled solver used in the simulations is based on a damped Newton method, yielding at convergence a weighted relative error of the solution of  $10^{-5}$ .

**3. Results.** The distribution of the magnetic induction, the current density and the azimuthal component of the Lorentz force in the vicinity of the hydrogen bubble obtained from the simulation are shown in Fig. 2. At the electrode surface, the modulus of the magnetic induction is 181 mT, which is in very good agreement with the measured value of 180 mT [11]. Fig. 3 shows in the top picture the color surface of the azimuthal velocity and vectors of the meridional velocity obtained when a slip condition at the interface is applied. The azimuthal velocity is in good agreement with the experimental result [11] and amounts to about 7 mm/s maximum. It also shows a differential rotation of the gas bubble interface which could influence the departure behavior. In comparison, the meridional convection is weaker in amplitude and is dominated by the respective secondary flow of the convection forced by the Lorentz force.

On the lower part of Fig. 3, the corresponding pressure surface shows a low-pressure region at the bubble foot. Fig. 4 shows the comparison of the pressure distribution  $p - p_c$  along the bubble interface for the slip and no-slip condition, where  $p_c$  denotes the respective pressure value at the electrode. Neglecting the motion of the interface clearly leads to an underestimation of the pressure maximum, as the electrolyte convection is damped near the interface. For the slip condition,

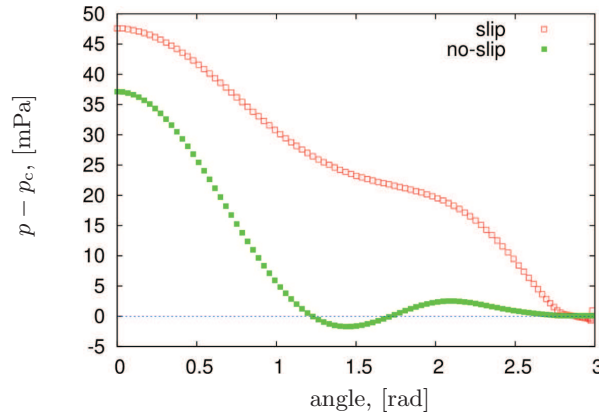


Fig. 4. Pressure distribution along the bubble surface (the angle increases from top (0) down to the contact point ( $\approx 3$ )) for different boundary conditions.

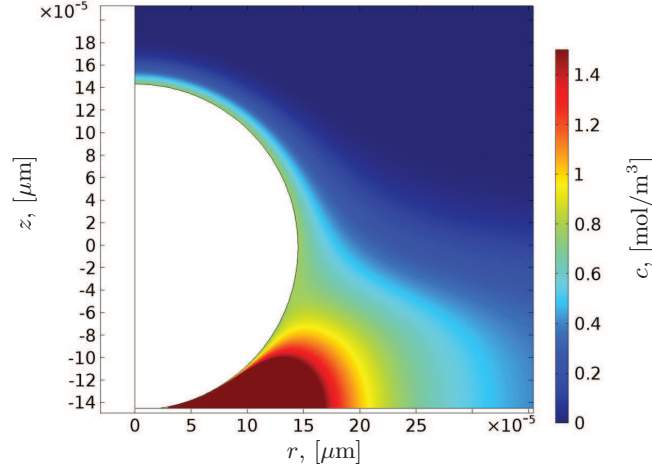


Fig. 5. Concentration of dissolved hydrogen in the vicinity of the gas bubble. The maximum value shown was restricted by hand.

the pressure difference between top and bottom amounts to about 48 mPa. Integrating  $p - p_c$  along the interface leads to a pressure force of about  $1.56 \times 10^{-9}$  N. The corresponding buoyancy force amounts to  $1.2 \times 10^{-7}$  N, which is almost 100 times larger than the pressure force, and also the capillary force is much larger. Therefore, the influence of the pressure force on the bubble departure can be assumed to be rather weak.

Fig. 5 shows the concentration of the dissolved hydrogen in the vicinity of the bubble. As expected, the maximum concentration is found in the lower region near the place of production at the wetted cathode part. Therefore, the growth of the gas bubble occurs mainly due to the mass transfer at the lower part of the interface. At the same time, a slow mass loss at the upper regions can be expected due to the mass transfer of hydrogen into the unsaturated electrolyte, analyzed in detail in [12].

**Conclusions.** The numerical results obtained give additional insight into the process of hydrogen electrolysis at a micro-electrode in a vertical magnetic field. The azimuthal convection driven by the Lorentz force agrees quantitatively with recent experimental results [11] and also qualitatively with the numerical results in [9] obtained at a higher value of the current density. The azimuthal motion of the bubble interface, shown here for the first time, could possibly enhance the bubble release by shear, although this can not be quantified at present. In contrast, the pressure force at the micro-electrode retards the bubble release. However, this force, even when taking into account a slip condition at the interface, is found to be small in comparison with other forces involved.

The amount and the direction of mass transfer of hydrogen along the bubble interface strongly vary. The concentration gradient of hydrogen along the bubble surface (see Fig. 5) may also drive a Marangoni flow, as hydrogen as a surfactant is known to influence surface tension [15]. This is left to future investigation. Further numerical results on the mass transfer of an electrochemically generated hydrogen bubble dissolving at a micro-electrode are reported in [12]. The quantitative influence of the Lorentz force on the integral mass transfer still needs to be investigated. Regarding the bubble departure, in our experiments, the effect of

a vertical magnetic field is found to be relatively weak, and further investigations will be useful here as well.

**Acknowledgments.** Financial support from DFG (DB, CC: Emmy-Noether grant No. CI 185/3; FK, MU: project TS 311/2-1; XY, KE: Ec201/4-1) is gratefully acknowledged.

## References

- [1] H. MATSUSHIMA *et al.* Gas bubble evolution on transparent electrode during water electrolysis in a magnetic field. *Electrochim. Acta*, vol. 100 (2013), pp. 261–264.
- [2] D. FERNANDEZ *et al.* Influence of magnetic field on hydrogen reduction and co-reduction in the Cu/CuSO<sub>4</sub> system. *Electrochim. Acta*, vol. 55 (2010), pp. 8664–8672.
- [3] J. KOZA *et al.* Hydrogen evolution under the influence of a magnetic field. *Electrochim. Acta*, vol. 56 (2011), pp. 2665–2675.
- [4] D. FERNANDEZ *et al.* Stabilizing effect of a magnetic field on a gas bubble produced at a microelectrode. *Electrochem. Comm.*, vol. 18 (2012), pp. 28–32.
- [5] H. LIU *et al.* Hydrogen bubble growth at micro-electrode under magnetic field. *J. Electroanal. Chem.*, vol. 754 (2015), pp. 22–29.
- [6] T. WEIER *et al.* Über die Lorentzkraft-getriebene dreidimensionale Strömung um eine magnetische Kugel in einem elektrischen Feld (Fachtagung “Lasermethoden in der Strömungsmesstechnik”, 8.–10. Sept. 2015, Dresden).
- [7] D. FERNANDEZ *et al.* Bubble formation at a gas-evolving microelectrode. *Langmuir*, vol. 30 (2014), pp. 13065–13074.
- [8] X. YANG *et al.* Dynamics of single hydrogen bubbles at a platinum micro-electrode. *Langmuir*, vol. 31 (2015), pp. 8184–8193.
- [9] H. LIU *et al.* Numerical simulation of hydrogen bubble growth at an electrode surface. *Can. J. Chem. Eng.*, vol. 94 (2016), pp. 192–199.
- [10] D. BACZYMAŁSKI *et al.* Near-wall measurements of bubble- and Lorentz-force-driven convection at gas-evolving electrodes. *Exp. Fluids*, 56 (2015), 162.
- [11] D. BACZYMAŁSKI *et al.* On the electrolyte convection around a hydrogen bubble evolving at a microelectrode under the influence of a magnetic field. *J. Electrochem. Soc.*, vol. 163 (2016), pp. E248–E257.
- [12] F. KARNBACH *et al.* Interplay of the open circuit potential-relaxation and the dissolution behavior of a single H<sub>2</sub> bubble generated at a Pt microelectrode. *J. Phys. Chem. C*, vol. 120 (2016), pp. 15137–15146.
- [13] T. IIDA *et al.* Water electrolysis under a magnetic field. *J. Electrochem. Soc.*, vol. 154 (2007), pp. E112–E115.
- [14] R. CLIFT *et al.* *Bubbles, Drops and Particles* (Dover Publ. Inc, Mineola, New York, 2005.)
- [15] S. LUBETKIN. Thermal Marangoni effects on gas bubbles are generally accompanied by solutal Marangoni effects. *Langmuir*, vol. 19 (2003), pp. 10774–10778.